

Stable configurations of confined cold ionic systems

(ion traps/crystallized ions)

ROBERT RAFAC*†, JOHN P. SCHIFFER*†, JEFFREY S. HANGST*†, DANIEL H. E. DUBIN‡,
AND DAVID J. WALES§

*Physics Division, Argonne National Laboratory, Argonne, IL 60439; †The University of Chicago, Chicago, IL 60637; ‡Department of Physics, University of California, San Diego, La Jolla, CA 92093; and §Department of Chemistry, University of Cambridge, Cambridge CB2 1EW, United Kingdom

Contributed by John P. Schiffer, September 4, 1990

ABSTRACT The simple structures formed by charged particles confined in a harmonic potential have been investigated and the configurations of minimum potential energy were identified. For fewer than 12 particles these form polyhedrons centered on the origin. For structures with 13–22 particles one sits in the middle, for 23–26 particles two are in the interior, etc., until a third shell starts forming at 60. When the isotropy of the trap is changed, distortions and discrete phase changes are seen. These structures should correspond to ones formed in ion traps at very low temperatures.

Systems of cold ions settle into stable configurations whose shapes depend only on the confining potential and the inter-ionic Coulomb forces. The nature of these configurations has been considered previously, at least since the time of J. J. Thompson's classical model of the atom (1, 2). With recent advances in the techniques of trapping and cooling ion clouds, such systems have become accessible to experimental investigation. At very low internal temperatures, the ions arrange themselves into symmetric crystalline arrays, a process that can be observed in laboratory ion traps of both the Penning (3) and Paul (4, 5) types. This followed early studies of charged Al particles suspended in a radio-frequency field by Langmuir and coworkers (6).

A number of calculations have addressed the problem of finding the configuration of minimum potential energy (CME) for various types of external confining potentials. In particular, several have published results on the CME for a small cloud of ions ($N < 30$) stored in an isotropic harmonic potential, but disagreements remain (7–9). The main purpose of the present note is to identify these configurations and so resolve some of the discrepancies in the literature. Furthermore, because some experimental work has also been performed for nonisotropic harmonic potentials, we explore how some of the minimum energy configurations change as the symmetry of the external harmonic potential varies.

The problem is one of classical physics; the dimensions are large compared to the wavelength of the ions. Since the number of degrees of freedom in these "Coulomb crystals" is large even for few ions, all but the most symmetrical configurations are studied here using numerical techniques. We apply several such methods, including molecular dynamics and Monte Carlo simulations, as well as direct multidimensional numerical minimization of the potential energy. The minimum configurations from the various methods were always consistent with each other.

The strengths of confining potentials commonly used in ion traps produce ion clouds with interparticle spacings on the order of a few to tens of micrometers, and the confining

potential is approximately harmonic (4, 5). The total potential energy of a cold system of N ions is then

$$U(r_1, r_2, \dots, r_N) = q^2 \sum_{i=1}^N \left\{ \sum_{j < i}^N \frac{1}{|r_i - r_j|} + \frac{1}{2d^3} [z_i^2 + \alpha(x_i^2 + y_i^2)] \right\}, \quad [1]$$

where the positions of the ions are given by $r_i = (x_i, y_i, z_i)$, ($i = 1, \dots, N$), q is the ionic charge, $d = (q^2/m\omega^2)^{1/3}$ is the unit length in a spherically symmetric harmonic potential of natural frequency ω for charged particles of mass m . The "trap parameter" α determines the symmetry of the external harmonic potential. Although in general it is possible to have different natural frequencies in the three directions, experiments have so far concentrated on the spherically symmetric ($\alpha = 1$) and cylindrically symmetric ($\alpha \neq 1$) cases.

Our molecular dynamics program is derived from that used (10) in the investigation of possible order in heavy-ion storage rings, where both two- and three-dimensionally confined many-particle systems were studied. For a given number of ions, each molecular dynamics calculation was started at a high temperature, then the system was slowly damped until a very low temperature was attained. In terms of the plasma parameter $\Gamma = (q^2/a)/kT$ (where kT is the temperature of the cloud and a is the interion spacing), all systems began with $\Gamma < 1$ and cooled to $\Gamma > 2 \times 10^5$; an infinite homogeneous plasma has been shown to crystallize into a body-centered cubic lattice (11–13) at $\Gamma \approx 178$ (14).

At the end of a complete run, the total potential energy of the system was stable to a few parts in 10^3 for the most flexible systems and typically a few parts in 10^4 for the more rigid ones. Initial configurations were varied to check that the final ordering was indeed the lowest one and not a local minimum. This procedure was found to be particularly important for $N > 19$, where many ions must simultaneously change positions to get from a local minimum to the global one, and the local minima are very closely spaced in energy. Further, geometric optimizations (constrained and unconstrained) were performed on many of the structures to verify that the true minimum in the potential energy was indeed achieved.

The Monte Carlo algorithm, used principally for $N \leq 10$ and $\alpha \neq 1$, moves ions randomly with a given step size δx and keeps the move only if the energy of the configuration is reduced. As a minimum in U is approached, δx is reduced to improve convergence until changes in the energy fall below a critical value. Up to 50 randomly generated initial conditions were used to make reasonably certain that all possible local minima were found. A conjugate gradient algorithm (15) was also employed in some cases to further improve the accuracy of the minimum energy configurations found from

The publication costs of this article were defrayed in part by page charge payment. This article must therefore be hereby marked "advertisement" in accordance with 18 U.S.C. §1734 solely to indicate this fact.

Abbreviation: CME, configuration of minimum potential energy.

the Monte Carlo method; final accuracies in the minimum energy were a part in 10^7 or better.

Finally, in some simple cases the minimum energy configurations were calculated analytically. In particular, we considered the cases $N = 2, 3$, and 4. Analytic results are presented whenever they are available.

The minimum energy configurations for systems with 2 to 15 ions in a spherically symmetric confining potential are given in Table 1 and shown in Fig. 1. It is evident that a number of the configurations do not agree with intuitive expectations. For example, when $N = 8$, the ions do not lie on the vertices of a cube but form two squares rotated by 45° with respect to each other (7), their respective centers separated by a distance 0.979 times their edge. Earlier publications incorrectly identified the "centered" tetrahedron (i.e., a tetrahedron with a fifth particle at its center) as the global minimum for five particles (9), the centered octahedron for seven (9), the cube for eight (8, 9), and the centered cube for the system of nine ions (9). Once the true minimum is known, it becomes fairly obvious that the other configurations are saddle points on the potential energy sur-

face—some have been included in Table 1 with some configurations that correspond to local energy minima. Note that shapes in which there is a rotational symmetry axis through each atom are guaranteed by symmetry to be stationary points of some order because there can be no resultant tangential force on any atom (16, 17). Methods of constrained optimization were employed to characterize these saddles, and some transition states were explicitly optimized using the Cerjan–Miller eigenvector-following method (18, 19).

Searches for true transition states (with precisely one negative force constant) were also conducted using the Cerjan–Miller method. The energies and geometries of these structures are important in interpreting the results of dynamical simulations and also provided interesting comparisons with the corresponding results for van der Waals clusters. For example, we found that Lipscomb's diamond-square-diamond process (20) was the predominant low-energy pathway for single-shell rearrangements, just as it is in small Lennard-Jones clusters and main group ligated clusters such as borohydrides (19).

Table 1. Summary of configurations of simple systems

Number of particles	Geometric description	Total potential energy	Radius	Interparticle spacing		
				a	b	c
2	Dumbell	1.191	0.629	1.258 (1)		
3	Equilateral triangle	3.120	0.833	1.443 (3)		
4	Tetrahedron	5.670	0.972	1.587 (4)		
5	Trigonal bipyramid	8.910	1.090	1.544 (6)	1.872 (3)	
(4+1)	Tetrahedron (+1)*	9.264	1.242	2.029 (4)		
6	Octahedron	12.639	1.185	1.676 (12)		
(5+1)	Trigonal bipyramid (+1)*	13.049	1.319	1.866 (6)	2.279 (3)	
7	Pentagonal bipyramid	17.024	1.273	1.508 (5)	1.790 (10)	
(6+1)	Octahedron (+1)*	17.296	1.386	1.960 (12)		
8	Square skew-prism	21.864	1.350	1.581 (8)	1.738 (8)	
	Cube*†	21.913	1.351	1.560 (12)		
9	3-Capped triangular prism	27.214	1.419	1.742 (12)	1.989 (6)	2.477 (3)
(8+1)	Square skew-prism (+1)‡	27.448	1.512	1.771 (8)	1.947 (8)	
(8+1)	Cube (+1)*	27.492	1.513	1.748 (12)		
10	2-Capped square skew-prism	33.058	1.484	1.600 (8)	1.621 (8)	1.898 (8)
11	Polyhedron	39.404	1.545			
12	Icosahedron	46.088	1.600	1.682 (30)		
(11+1)	Polyhedron (+1)‡	46.234	1.674			
13 (12+1)	Icosahedron (+1)	53.312	1.721	1.810 (30)		
(13)	Polyhedron‡	53.364	1.654			
14 (13+1)	Polyhedron (+1)	60.959	1.768			
15 (14+1)	2-Capped hexagonal skew-prism (+1)	68.958	1.812	1.616 (12)	1.851 (12)	1.884 (12)
16 (15+1)	Polyhedron (+1)	77.382	1.855			
17 (16+1)	2-Capped hexagonal skew-prism (+1)	86.201	1.895			
18 (17+1)	7-Capped pentagonal prism (+1)	95.418	1.934			
19 (18+1)	Polyhedron (+1)	105.022	1.973			
20 (19+1)	Polyhedron (+1)	115.042	2.009			
21 (20+1)	Polyhedron (+1)	125.381	2.044			
22 (21+1)	Polyhedron (+1)§	136.120	2.079			
23 (21+2)	Polyhedron (+2)	147.202	2.152			
24 (22+2)	Polyhedron (+2)	158.624	2.183			
25 (23+2)	Polyhedron (+2)	170.415	2.214			
(22+3)	Polyhedron (+3)¶	170.426	2.249			
26 (24+2)	Polyhedron (+2)	182.512	2.243			
27 (24+3)	Polyhedron (+3)	194.955	2.307			

Unless otherwise noted, all values pertain to the configuration of minimum energy. Units of distance and energy are as discussed in the text. Under number of particles, some configurations suggested by others as having minimum energy are indented, and where some particles are in the center, the parentheses give the number in the outer polyhedron + the number in the center. Under geometric description, the number of particles in the interior is given in parentheses. For interparticle spacing, the number of times a particular spacing occurs in the structure is given in parentheses.

*Configurations erroneously assigned as the configuration of minimum energy in ref. 9.

†Configurations erroneously assigned as the configuration of minimum energy in ref. 8.

‡Refers to a configuration that is a local minimum.

§We are indebted to R. Hasse for pointing out to us the correct configuration of minimum energy for 22 ions.

¶Configuration with a different radius incorrectly assigned as the configuration of minimum energy in ref. 7.

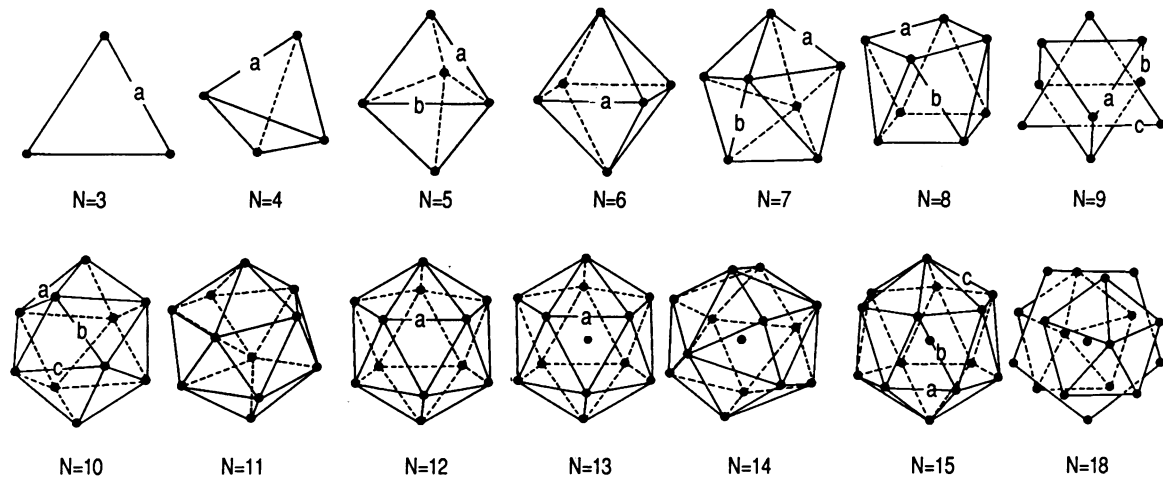


FIG. 1. Configurations of some of the simplest ionic systems in isotropic confinement. The lines are drawn to emphasize groups of ions that form simple geometrical shapes. The letters refer to distances that are shown in Table 1.

Ref. 8 reported no definite minimum-energy configuration for systems of seven and nine ions; however, we do not find this to be the case. The minima for these systems do not appear qualitatively different from the others, these systems are not particularly flexible or in unusually shallow minima, nor did repeated heating/cooling cycles in the molecular dynamics method change the final configurations.

Table 1 also lists the energies and mean nearest-neighbor distances for some systems with $N > 15$.

In the simulation of large ionic systems, it had been found (10, 13, 21, 22) that cold ion clouds arrange themselves in layered structures, and for isotropic confinement these take the form of concentric spherical shells. Such shell structure has been confirmed experimentally (3). We have investigated the onset of the formation of shells in small systems. As can be seen from the tables, the polyhedral structure of the ionic configuration evolves in a straight-forward fashion until $N = 13$, where it becomes energetically favorable to have a single ion inside the shell. For $22 < N < 27$, there are two ions inside the outer envelope, etc. Near the transition from n to $n + 1$ ions inside the shell, there are local minima that may have one extra or one fewer ion within the outer shell. For instance, the case of $N = 25$ was erroneously reported (7) to have three ions in the center with energy $U = 170.426$; the actual global minimum has two central ions and $U = 170.415$.

For large N , the multitude of possible orderings makes it more difficult to unambiguously locate the configuration that represents the true minimum in potential energy. However, we have found that the local minima fall into classes that are qualitatively similar in appearance and that have very closely spaced energies; they may be classified according to the number of ions in each shell. For instance, we find that for the 60-ion system the minimum energy is for a configuration consisting of an icosahedron surrounded by a 48-ion outer shell, having total potential energy $U = 774.511$. It also appears that the $N = 61$ system is the first with a particle appearing in the middle of the inner shell—the beginning of a third shell with the outer two shells in the same shape as found for 60 ions and a total potential energy $U = 796.721$. The pattern continues; the 62-ion system has a 13-ion inner shell with 1 central ion, 63 ions have a 14-ion inner shell with 1 central ion, and 64 ions have a 15-ion inner shell with 1 central ion. These three configurations seem to be the true minima with energies of 819.236, 841.942, and 864.937, respectively; however, there are a number of local minima all within a few parts in 10^5 of each of the quoted values.

The inner-shell structures obtained are analogous in shape to those for the corresponding number of ions confined alone.

The configurations of inner-shell ions, however, have slightly larger radii than the same free structures—they are slightly attracted to the “holes” in the next shell. Table 2 gives a comparison of these configurations for a few such systems.

For $N = 100$ (a case studied in ref. 22), all of the local minima were qualitatively similar to those observed previously: there were three concentric shells with 4, 26, and 70 ions, and the lattice structure within the outer shells was the distorted two-dimensional hexagonal lattice that is the characteristic arrangement on the layered surfaces of larger systems (10, 22). These observations can be explained using idealized models for the cloud's lattice structure (23). The models lead to an estimate that up to 60 concentric shells may be required before the interior of the cloud takes on a body-centered cubic lattice structure (i.e., the structure of an infinite system).

The radius of the configuration changes relatively smoothly with the total number of particles, as may be noticed in Fig. 2 where the mean radius divided by the arbitrary factor $N^{0.4687}$ is displayed. Some discontinuities are evident. For instance, the emergence of an inner ion in the 13-ion configuration increases the radius of the outer icosahedron by 7.6%. Analogously, more than 1 ion inside the shell volume causes the outer shell to become deformed by a small amount along the symmetry axis of the internal structure. The two ions in systems with $22 < N < 27$ deform the outer shell along the dumbbell axis causing it to be 4–5% larger along the axis than perpendicular to it. For the 27-particle configuration, which has an equilateral triangle within the shell volume, the radius is $\approx 4.5\%$ larger in the plane of the triangle than perpendicular to it.

For an anisotropic confinement ($\alpha \neq 1$ in Eq. 1), it is evident that the configuration of lowest energy will change. We find that as the trap parameter α is varied continuously, the CME also changes continuously except at specific α values at which jumps in the symmetry of the CME occur.

Table 2. Comparison of some simple structures with the analogous structure surrounded by an outer shell

Number of particles in structure	Number of particles in surrounding shell	Radius of configuration*	Radius of same configuration when surrounded by a shell*
3	24	0.833	0.997
12	48	1.600	1.607
12 + 1	48	1.721	1.733
14 + 1	48	1.812	1.823

*Units of distance are as discussed in the text.

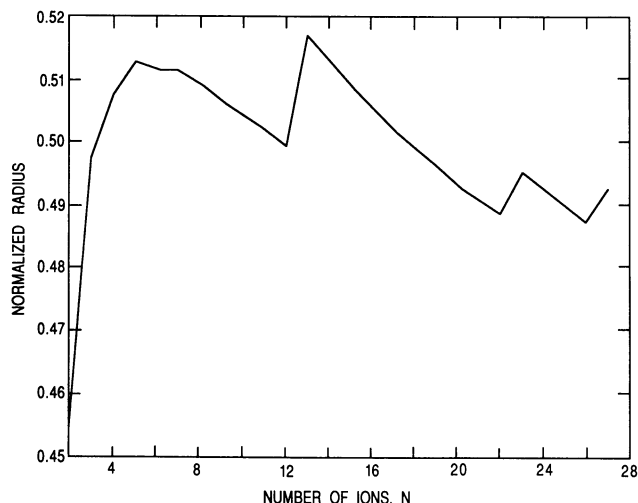


FIG. 2. Mean radius of ions in the outer shell for isotropic confinement plotted as a function of the number of ions N in the cloud. This radius is divided by $N^{0.4687}$ (the power that approximately compensates for the average increase with ion number). The discontinuities at 13 and 22 ions correspond to the appearance of 1 and 2 ions in the interior of the cloud, respectively.

These jumps are due to competing local energy minima, which become lowest energy at these α values. The transitions are similar to the structural phase transitions of charges confined to move on simple surfaces (24). They can be classified according to the type of discontinuous change in a symmetry parameter (the mean cloud radius $\langle r \rangle$, for example): some behave like first-order transitions ($\langle r \rangle$ has a discontinuity) and some behave like phase transitions of the second kind (derivatives of $\langle r \rangle$ with respect to α are discontinuous). Furthermore, as was previously noted for the spherical case, there can be more than one stable local minimum at a given α value. Stability of a given equilibrium has been studied by numerical determination of the spectrum of normal mode frequencies. When one or more of the frequencies becomes imaginary, the equilibrium is no longer stable. In the following cases, the range of α values over which a given configuration is stable is the same as the range over which the configuration is the CME, except where specifically stated otherwise.

The case of $N = 2$ is trivial; for $\alpha < 1$ the ions sit on opposite sides of the origin in the x - y plane; the distance between the ions is $(2/\alpha)^{1/3}$. For $\alpha > 1$ the ions are aligned along the z axis; the distance between them is $2^{1/3}$. These are the only stable configurations. The point $\alpha = 1$ is special in that any rotation of the configuration around the origin is allowed; this rotational symmetry occurs for all N values.

For $N = 3$, three configurations are stable, again with nonoverlapping regimes of stability. For $\alpha < 1$, the ions form an equilateral triangle in the x - y plane with sides of length $(3/\alpha)^{1/3}$. For $1 < \alpha < 12/5$, the ions form an isosceles triangle with the long side parallel to the z axis; for $\alpha > 12/5$, the ions are squeezed onto the z axis; the distance between the ions is $(5/4)^{1/3}$.

As N increases the observed minimum energy structures become ever more complex. For example, for $N = 4$, six distinct symmetries are found; they have nonoverlapping regimes of stability except in configurations *ii* and *iii*, which are both stable in the range $1.40 < \alpha < 1.63$.

(i) For $0 < \alpha < (1 + 2^{2/3})/2^{5/2} = 0.677$ all four particles are in the x - y plane, forming a square.

(ii) For $0.677 < \alpha < 1.4705$ (stable for $0.677 < \alpha < 1.6279$), the configuration is no longer coplanar; it becomes a tetra-

hedron with two equal-length edges that are perpendicular to and bisected by the z axis.

(iii) For $1.4705 < \alpha < 2 \times 3^{3/2}/(1 + 3^{3/2}) = 1.677$ (stable for $1.4019 < \alpha < 1.677$), the tetrahedron now has one edge parallel to the z axis and one perpendicular.

(iv) For $1.677 < \alpha < 2.8468$, the configuration becomes a coplanar parallelogram with two ions on the z axis and two in the x - y plane.

(v) For $2.8468 < \alpha < 4.1542$, the parallelogram is squeezed so that the ions previously in the x - y plane move out of the plane, one falling above and the other below.

(vi) For $4.1542 < \alpha < \infty$, the ions are squeezed onto the z axis with the spacing between the inner pair 0.9250 times that between the outer ones.

For larger values of N the CMEs become more numerous and complex as a function of α . They have been determined numerically for $N \leq 10$; an interactive graphics representation of the CMEs for $3 \leq N \leq 10$, which can be run on a Macintosh computer, is available upon request.[¶]

In general as $\alpha \rightarrow \infty$, the configuration becomes a line along the z axis with the number of ions per unit length scaling for large N as $1 - (z/z_0)^2$ (where z_0 is half the length of the line of charges). As $\alpha \rightarrow 0$ the cloud settles into the x - y plane and forms a distorted two-dimensional hexagonal lattice with the number of ions per unit area scaling for large N as $[1 - (r/r_0)^2]^{1/2}$ (where r_0 is the radius of the cloud).

To summarize, the symmetrical shapes seen for cold ionic systems in an isotropic harmonic well go through a variety of simple shapes that change when the confining well deviates from isotropy. Many aspects of the symmetries and the dynamics of ions in ion traps are likely to be influenced by more detailed study of these configurations.

[¶]Mail a self-addressed envelope together with a blank 3.5-inch diskette to D. Dubin, address as above.

This research was supported by the U.S. Department of Energy, Nuclear Physics Division, under Contract W-31-109-Eng-38; as well as the National Science Foundation, under contract PHY87-06358; the U.S. Office of Naval Research, under Contract N00014-89J-1714; and the San Diego Supercomputer Center.

1. Thompson, J. J. (1904) *Phil. Mag.* **S.6** 7, 237-265.
2. Thompson, J. J. (1921) *Phil. Mag.* **S.6** 41, 510-544.
3. Gilbert, S. L., Bollinger, J. J. & Wineland, D. J. (1988) *Phys. Rev. Lett.* **60**, 2022-2025.
4. Wineland, D. J., Bergquist, J. C., Itano, W. M., Bollinger, J. J. & Manney, C. H. (1987) *Phys. Rev. Lett.* **59**, 2935-2938.
5. Diedrich, F., Peik, E., Chen, J. M., Quint, W. & Walther, H. (1987) *Phys. Rev. Lett.* **59**, 2931-2934.
6. Wuerker, R. F., Shelton, H. & Langmuir, R. V. (1959) *J. Appl. Phys.* **30**, 342-349.
7. Mostowski, J. & Gajda, M. (1985) *Acta Phys. Pol. A* **67**, 783-802.
8. Casdorff, R. & Blatt, R. (1988) *Appl. Phys. B* **45**, 175-182.
9. Baklanov, E. V. & Chebotayev, V. P. (1986) *Appl. Phys. B* **39**, 179-181.
10. Rahman, A. & Schiffer, J. P. (1986) *Phys. Rev. Lett.* **57**, 1133-1136.
11. Brush, S., Sahlin, H. L. & Teller, E. (1966) *J. Chem. Phys.* **45**, 2102-2118.
12. Pollock, E. L. & Hansen, J. P. (1973) *Phys. Rev. A Gen. Phys.* **8**, 3110-3122.
13. Dubin, D. (1990) *Phys. Rev. A Gen. Phys.*, in press.
14. Stringfellow, G. S., DeWitt, H. E. & Slattery, W. L. (1990) *Phys. Rev. A Gen. Phys.* **41**, 1105-1111.
15. Press, W. H., Flannery, B. P., Teukolsky, S. A. & Vetterling, W. T. (1986) in *Numerical Recipes: The Art of Scientific Computing* (Cambridge Univ. Press, New York), pp. 301-306.
16. Leech, J. (1957) *Math. Gazette* **41**, 81.
17. Wales, D. J. (1990) *J. Am. Chem. Soc.*, in press.
18. Cerjan, C. J. & Miller, W. H. (1981) *J. Chem. Phys.* **75**, 2800-2806.
19. Wales, D. J. (1989) *J. Chem. Phys.* **91**, 7002-7010.
20. Lipscomb, W. N. (1966) *Science* **153**, 373-378.
21. Schiffer, J. P. (1988) *Phys. Rev. Lett.* **61**, 1843-1846.
22. Dubin, D. H. E. & O'Neil, T. M. (1988) *Phys. Rev. Lett.* **60**, 511-514.
23. Dubin, D. H. E. (1989) *Phys. Rev. A Gen. Phys.* **40**, 1140-1143.
24. Berezin, A. A. (1985) *Am. J. Phys.* **54**, 403-405.